Azimuthal Dipolar Rotor Arrays on Surfaces

Sebastian Hamer,[a] Jan-Simon von Glasenapp,[a] Fynn Röhricht,[a] Chao Li,[b] Richard Berndt,[b] and Rainer Herges*[a]

Dedicated to Prof. Dr. Klaus Hafner

Abstract: A set of dipolar molecular rotor compounds was designed, synthesized and adsorbed as self-assembled 2D arrays on Ag(111) surfaces. The title molecules are constructed from three building blocks: (a) 4,8,12-trioxatriangulene (TOTA) platforms that are known to physisorb on metal surfaces such as Au(111) and Ag(111), (b) phenyl groups attached to the central carbon atom that function as pivot joints to reduce the barrier to rotation, (c) pyridine and pyridazine units as small dipolar units on top. Theoretical calculations and scanning tunneling microscopy (STM) investigations hint at the fact that the dipoles of neighboring rotors interact through space through pairs of energetically favorable head-to-tail arrangements.

Introduction

Molecular rotors are fundamental parts in artificial molecular machines[1,2] and in a number of biological systems.[3,4] Besides the investigation and construction of individual, molecular functional units, the coupling of ensembles of rotors in 2D and 3D arrays is intriguing from a fundamental and an application oriented point of view.[5,6,7]

A number of different strategies were developed to mount rotor-type molecules on surfaces. Hla et al. adsorbed isolated rotor structures on Au(111) surfaces that are either mounted on molecular tripods attached to the gold surface through thioethyl groups[8] or a substituted cyclopentadienyl moiety[9] while a Ru atom serves as a pivot joint. A number of sandwich (double-decker) complexes have been investigated as rotors on surfaces.[10,11,12,13] Mechanically interlocked rotors have also been shown to perform gear-like rotation.[14] However, these examples focus on two or a limited number of neighboring rotors.

While remaining overall scarce, there are several reports on ordered 2D rotor arrays. Phthalocyanines[15] or sandwich complexes of porphyrins[13] or phthalocyanines[10,16] containing lanthanoid metals form self-assembled arrays of rotors on Au(111) surfaces. Rotors with permanent dipole moments may exhibit spontaneous, collective orientation of their dipole moments through through-space dipole-dipole interaction, and they may be addressed through external stimuli such as electric fields and manipulation through an STM tip.[16,17,18] A recent publication reports on molecular rotors with a dipolar head group mounted on a molecular tripod.[19] STM manipulation of the dipolar group leads to correlated motion of neighboring molecules. Ordered arrays of dipolar rotors could thus lead to the fabrication of ferroelectric materials.[20] Such 2D dipolar rotor arrays on surfaces have already been found to undergo collaborative rotation and formation of domains when exposed to sufficiently high STM currents as shown by Rapenne, Hla et al. in a hexagonal network of porphyrin double decker complexes.[16]

Over the last decade, our group has established the so called platform approach.[21] As molecular platforms we employ triaza-triangulenium (TATA)[22] or trioxa-triangulenium (TOTA)[23,24] cations, which form self-assembled monolayers on Au(111) or Ag(111) surfaces. A variety of groups has been attached to the central carbon atom of the platforms, which are freestanding upright at a lateral distance defined by the size and the absorption pattern of the platforms underneath. Electronic coupling of the functional groups with the metal surface was tuned by introducing spacer groups of different lengths and π conjugation.[25] Particularly ethinyl and phenyl groups as spacers are suitable to increase the distance from the surface and allow for almost free rotation of the functional groups on top. A number of photoswitchable molecules, such as azobenzenes[26,27,28] and diazocines[29,30] were mounted onto TATA and TOTA platforms. The molecules were adsorbed on Au(111) and Ag(111) surfaces, and their switching behavior was investigated by STM. Whereas TATA based molecules are designed to form ordered monolayers from solution under ambient conditions, TOTA compounds have a higher propensity to sublime without decomposition in high vacuum, and are therefore ideal to prepare monolayers for low temperature,

[a] S. Hamer, J.-S. von Glasenapp, F. Röhricht, Prof. Dr. R. Herges
Otto-Diels-Institut für Organische Chemie
Kiel University
Otto-Hahn-Platz 4, 24098 Kiel, (Germany)
E-mail: rherges@oc.uni-kiel.de

[b] Dr. C. Li, Prof. Dr. R. Berndt
Institut für Experimentelle und Angewandte Physik
Kiel University
Leibnizstrasse 19, 24098 Kiel (Germany)

Supporting information for this article is available on the WWW under https://doi.org/10.1002/chem.202103237

high vacuum STM investigations.[31] Besides photoswitches,[32] polar molecules were attached to TOTA platforms[33] and their rotation was investigated by STM. Following this concept, platforms functionalized with dipolar rotors were used to create self-assembled arrays of rotors as shown schematically in Figure 1.

In this work, we present the synthesis of dipolar rotor functionalized platform molecules that self-assemble into ordered 2D arrays on Ag(111) surfaces (Figure 1). Phenyl spacers as pivot joints attached to the center of the platforms (grey spheres) allow for almost free rotation of the pyridine and pyridazine rings above (arrows with blue base and red arrowhead). Besides the dipolar rotors, a biphenyl compound which serves as a reference for STM experiments was also prepared as shown in Figure 2. The pyridazine units exhibit a dipole moment of 4.24 Debye parallel to the surface and interact with each other through space, forming characteristic patterns visible in the STM images. Pyridine units in comparison exhibit roughly half the dipole moment with 2.26 Debye (see Supporting Information, page S35). Theoretical calculations predict that pairs of dipoles form head-to-tail dimers. Coulomb attraction in these pairs are strong enough to bent the rotors towards each other to such an extent that hydrogen bonds are formed between the nitrogen lone pairs of pyridazine and a C–H bond of the neighboring molecule.

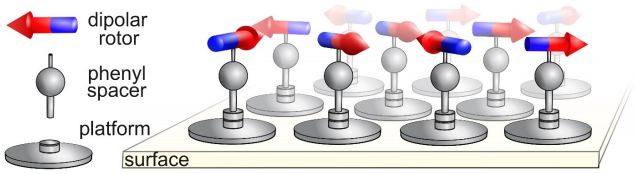

Figure 1. Schematic view of a self-assembled 2D dipolar rotor array on a surface, based on the platform concept. TOTA molecules were used as platforms, phenyl groups as pivot joints and pyridazine and pyridine as dipoles (blue arrows with red arrowheads). The dipoles interact through space with each other.

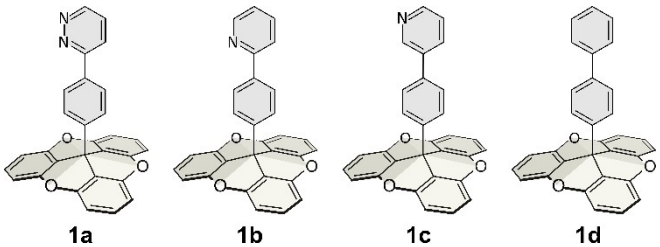

Figure 2. Structures of the synthesized dipolar rotor functionalized platforms **1 a–c** and a reference compound without dipole moment **1 d**.

Results and Discussion

Synthesis of the functionalized platforms 1 a–d

Key step in the synthesis of the dipolar rotor or biphenyl functionalized TOTA compounds is the polar C–C bond formation of the TOTA cation with the functional molecule on top, which acts as the nucleophile. The standard method to achieve this polar bond formation implies the use of lithium organic compounds generated by halogen metal exchange and reaction with the TOTA cation. However, the preparation of the lithium organic compounds by halogen metal exchange in this work gave rise to the formation of side products when applied to pyridazine derivatives and didn't lead to success. Therefore, a detour involving stannylated intermediates (**6**, Scheme 1), developed by Staubitz et al. was applied.[34] The iodine substituent in **5** was first converted to the corresponding trimethylstannyl group through a palladium catalyzed cross-coupling reaction with distannane (**5**→**6**). Selective exchange of the stannyl group with lithium is achieved by reaction with MeLi under mild conditions at low temperatures. The lithium compound generated in situ was reacted with the TOTA cation (**6**→**1**). Another problem leading to low yields is the poor solubility of the $TOTA^+$ BF_4^- salt, which is the product of the standard literature synthesis. To increase the solubility in organic solvents the $TOTA^+$ tetrakis-[3,5-bis-(trifluoromethyl) phenyl]-borate (BAr^F_4) salt **2** (Figure 3) was used, which is well soluble in organic solvents.[32] Another detour was necessary to prepare the biaryl iodide **5**. To avoid polymerization during the aryl-aryl coupling step, the bromide in the phenyl component was masked as a TMS group (**7**→**8**), which after Suzuki coupling (**3**→**4**) was replaced by iodine using I–Cl (**4**→**5**).

Starting from the halogenated heteroaromatics 3-chloropyridazine[35] (**3 a**) and commercially available 2- and 3-bromopyridine (**3 b**, **c**), cross coupling with 4-(trimethylsilyl)phenyl boronic acid pinacol ester (**8**) was performed. The boronic acid ester **8** was obtained through two subsequent lithiation/substitution steps of 1,4-dibromobenzene (**7**) in a one-pot reaction. The subsequent Suzuki reactions were accomplished in yields exceeding 90% using standard conditions, giving the *para*-trimethylsilylphenyl substituted heteroaromatics **4 a–c**. Iodination of these was achieved by *ipso* substitution of the TMS groups with iodine monochloride, producing the iodinated biaryls **5 a–c** in good yields. Subsequent stannylation of **5 a–d** was performed following the literature protocol[34] using hexamethyl distannane and palladium catalysis in a microwave

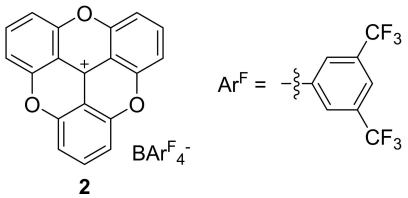

Figure 3. 4,8,12-Trioxatriangulenium (TOTA) cation was applied as the tetrakis[3,5-bis(trifluoromethyl)phenyl]-borate (BAr^F_4) salt **2**.

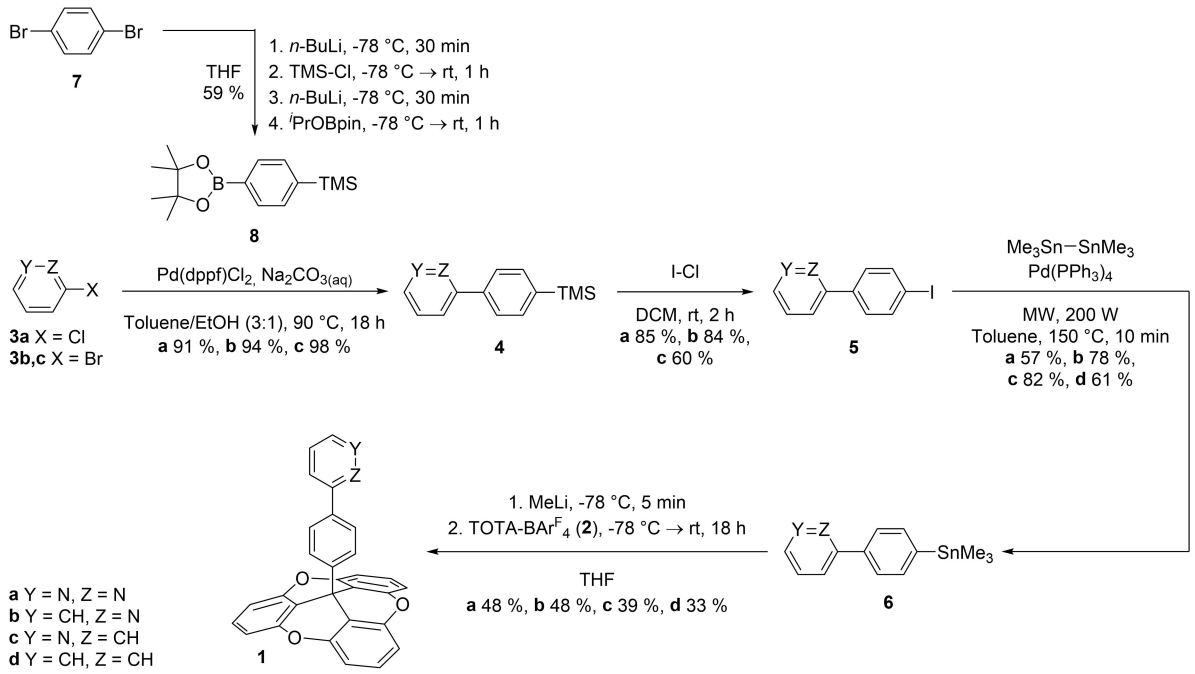

Scheme 1. Synthetic route for the preparation of the target compounds **1 a**–**d**.

reactor. This method was very convenient due to short reaction time and simple workup, yielding the stannylated compounds **5 a**–**d**. For the final connection of the TOTA cation and the dipolar rotor, the stannylated biaryls **6 a**–**d** were lithiated using methyllithium, followed by the addition of $TOTA^+$ $BAr^F_4{}^-$ (**2**) to obtain the funtionalized platform compounds **1 a**–**d** in yields up to nearly 50 %.

Preliminary results of STM measurements

The platform based dipolar rotor, 3-phenylpyridazine-TOTA (**1 a**) was sublimed in vacuo and deposited onto an Ag(111) surface (for details see Supporting Information). The molecules form monolayers that were investigated by STM (Figure 4,).

These first STM images reveal the formation of a self-assembled monolayer of **1 a** and allow to distinguish between intact compounds and fragmented, unfunctionalized TOTA-platforms on the surface. It was shown that it is possible to remove single molecules from the surface by STM voltage. We will comment further on the arrangement and those of the remaining compounds in future reports, yet we can already show the deposition of an intact azimuthal rotor network on a Ag(111) surface. An example of the manipulation of molecules at the edge of an island with the STM suggests that rotation may be induced (Figure 5). (Figure 5).

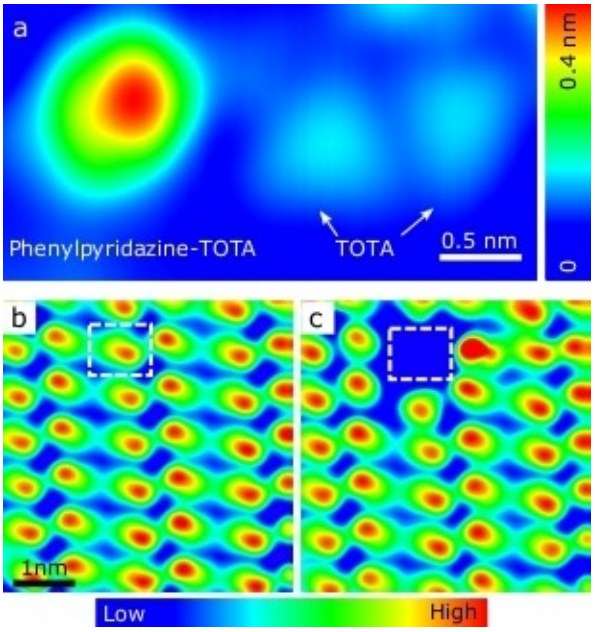

Figure 4. STM topographs of 3-phenylpyridazine-TOTA (**1 a**) sublimed onto Ag(111) recorded at a constant current I = 10 pA. The false color scales used are indicated. (a) Close-up view of an intact molecule (left) along with two $TOTA^+$ platforms (right). Sample voltage V = −0.1 V. (b) Self-assembled island imaged at V = 0.1 V. (c) The same island imaged again after applying a current pulse at an elevated sample voltage of 2.5 V over tens of seconds. The pulse led to the disappearance of a single 3-phenylpyridazine-TOTA (**1 a**) molecule from the network as indicated by a dashed frame.

Theoretical calculations

To obtain structural details and information about intramolecular and intermolecular interaction energies we performed quantum chemical calculations using Turbomole[36] at the PBE/def2SVP (DSP-D3-BJ) level of density functional theory. Unfortunately, arrays of dipolar rotors on surfaces as represented in the

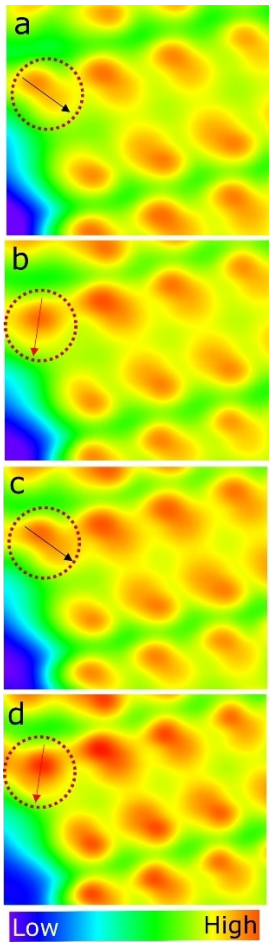

Figure 5. (a) STM image of the edge of a self-assembled island of phenyl-pyridazine-TOTA (**1 a**) on Ag(111). Manipulation experiments were performed on the molecule marked by a dashed circle. The initial orientation of the targeted molecule is indicated by an arrow. (b–d) Orientations of the targeted molecule after the first, second and third manipulation with the STM tip. The data suggest that the phenylpyridazine group is reversibly alternating between two orientations. Imaging parameters: I = 10 pA and V = 0.1 V. Manipulation procedure: The STM tip is initially placed next to a target molecule. Next, the tip is brought closer until I ~ 3 nA is reached at V ~ 5 mV, and then moved along the molecule at constant height. Finally, the tip is retracted to imaging conditions.

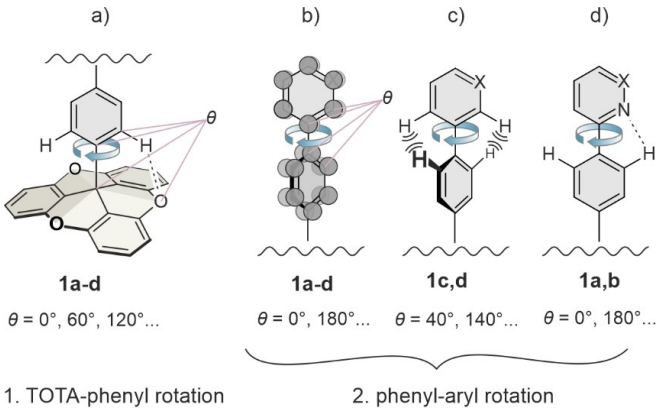

Figure 6. Four types of interactions that control the rotation of the dipolar rotor mounted on top of the platform. θ are the torsional angles defined by the 4 atoms indicated. a) H-bond between a C–H of the phenyl ring and the oxygen atoms of the TOTA platform, b) π conjugation, c) steric repulsion of the H atoms adjacent to the aryl-aryl bond, d) H bond between the phenyl C–H and the N atom of the rotor on top.

STM image (Figure 4) are too large systems to be calculated at an adequate level of theory. In our first attempts, we replaced the Ag(111) surface by a single layer of Ag atoms and performed calculations on isolated molecules and dimers on the silver slabs.

Assuming that the platform is fixed on the surface (stator), there are two C–C single bonds (1. TOTA-phenyl and 2. phenyl-aryl) that allow rotation of the dipole on top of the platform. The overall barrier to rotation of an isolated dipolar rotor is defined by four (weak) intramolecular interactions (a–d, Figure 6).

1. a) There is H-bond formation of the *ortho* hydrogens of the lower phenyl ring with the three oxygen atoms of the platform, which leads to a sixfold degenerate minimum on the rotational energy hypersurface (Figure 6a). The C–H···O hydrogen bond is weak and consequently, the rotational barrier with $\Delta H^{+} = 0.25$ kcal mol^{-1} is low (Supporting Information Figure S27). 2. The phenyl-aryl torsion is more intricate. In an ideal, unhindered biaryl system the two aromatic rings should be coplanar to maximize their π overlap (Figure 6b). However, the H atoms adjacent to the aryl-aryl bond experience a slight steric repulsion, which leads to a twist angle of about 40° (Figure 6c), which is a compromise between H···H repulsion and planarization driven by π conjugation. There are four energetically degenerate minima and two different transition states during a 360° rotation of the two phenyl rings with respect to each other. Two barriers at 0° and 180° ($\Delta H^{+} = 1.4$ kcal mol^{-1}) are due to maximum H···H repulsion and the transition states at 90° and 270° ($\Delta H^{+} = 2.7$ kcal mol^{-1}, Supporting Information Figure S28) define a complete loss of π conjugation at orthogonal orientation. Fortunately, the situation in the pyridazine-phenyl (**1 a**) and pyridine-phenyl torsion (**1 b**) is simpler (Figure 6d). There is only one pair of H atoms (instead of two as in biphenyl **1 d** and in **1 c**) that get into each other's way, and more importantly, there is an H bond between N atom in the pyridazine or pyridine ring with the adjacent H atom in the phenyl ring that acts as a driving force towards planarization (Figure 6d). Our calculations predict that the two aromatic rings in **1 a** and **1 b** are coplanar. There is a substantial barrier of 6 kcal mol^{-1} towards rotation (Supporting Information, Figure S28). As expected, the transition state structure exhibits two orthogonal aryl rings with a complete loss of π conjugation and rupture of the C–H···N hydrogen bond. As a bottom line we conclude that if there is an external force (e.g., from an STM tip or electrostatic interaction with a neighboring molecule) it will rather be the TOTA-phenyl bond ($\Delta H^{+} = 0.25$ kcal mol^{-1}) than the phenyl-pyridazine/pyridine bond ($\Delta H^{+} = 6.0$ kcal mol^{-1}) that rotates in **1 a** and **1 b**. The situation is more complicated in **1 c** and **1 d** (see Supporting Information).

Another force that controls the rotation of the dipoles and their orientation with respect to each other are the intermo-

lecular dipole-dipole interactions. To obtain a rough estimate about the strength of these electrostatic interactions, the distance between the dipoles on the surface must be known. Previous experiments with arrays of methyl-TOTA on Ag(111) revealed a next neighbor distance (distance of midpoints of two neighboring platforms) of ~10 Å. The energetically most favorable orientation of two platforms with respect to each other is edge to edge, forming two C–H···O hydrogen bonds (Figure 7). However, the attractive electrostatic forces between two adjacent dipoles could lead to shorter platform distances. To plot the potential energy as a function of the platform distance *d*, two phenylpyridazine-TOTA platforms (**1 a**) and as a reference two H-TOTA platforms were placed on a single sheet of silver atoms (Figure 7). For further information regarding the distance scan see Supporting Information.

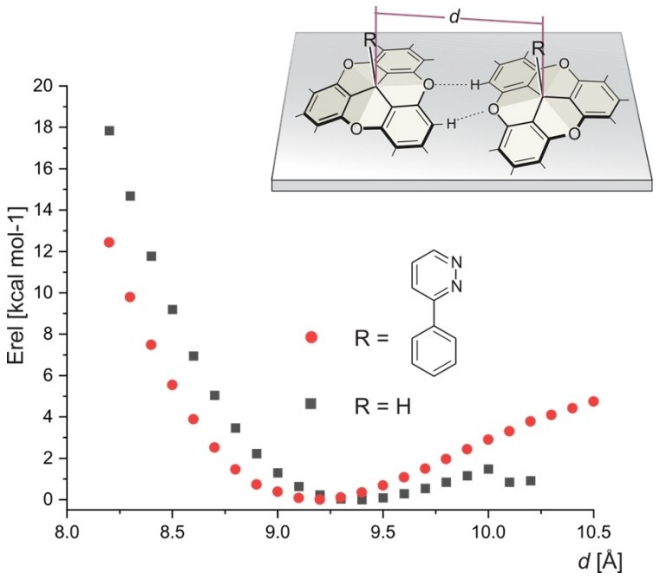

Figure 7. Distance scans of an H-TOTA and a pyridazine-TOTA dimer on a single layer of silver atoms (Ag(111) orientation). For H-TOTA the drop in energy at $d > 10$ Å correlates with a beginning transition from edge-to-edge to head-to-edge configuration.[24] Level of theory: PBE/def2SVP (DSP-D3-BJ). For more information see Supporting Information p. 34.

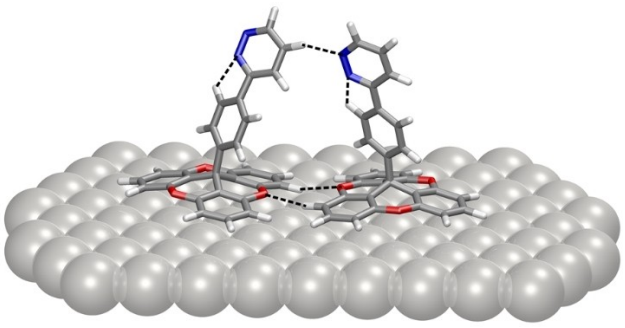

Figure 8. Structure of a pyridazine-TOTA dimer on a single layer of silver atoms. The silver layer was fixed at the geometry of bulk silver (Ag(111)). All other geometry parameters were optimized (PBE/def2SVP (DSP-D3-BJ). H-bonds are indicated with dashed lines.

The **1 a** dimer is most stable at a distance of $d = 9.15$ Å and the H-TOTA dimer at $d = 9.3$ Å. The energy minimum in both cases is due to the formation of two intermolecular C–H···O hydrogen bonds between the two platforms. The slightly shorter distance between the **1 a** platforms as compared to the H-TOTA dimer is due to an additional intermolecular C–H···N hydrogen bond between the two pyridazine rings on top of the two platforms. Whereas the phenyl-pyridazine unit in isolated platform molecules stand upright and orthogonal to the surface, the two biaryl units considerably bend towards each other to form an intermolecular hydrogen bond (Figure 8). Obviously, the electrostatic dipole-dipole interaction (head-to-tail orientation of the pyridazine units) and the concomitant formation of a C–H···N hydrogen bond are able to distort the four bond angles including the two C–C single bonds considerably. From our calculations, we infer that these intermolecular forces are at least one order of magnitude larger than the barriers of rotation. Hence, the dipole-dipole interactions should dominate the orientation of the pyridazine units, whereas the intrinsic barrier to rotation can be neglected as a first approximation.

To obtain more information about the correlated motion of the dipolar rotors in a dimer, we calculated the energy hypersurface of a dimer at a distance of d = 9.1 Å as a function of the two rotational angles θ_a *and* θ_b (Figure 9). These simplified model calculations confirm the head-to-tail arrangements as the global minima on the energy hypersurface (deep blue color in Figure 9). The transition between two different minima (rotation of both dipoles by 180°) follows a correlated motion through a T type orientation. The lowest energy path involves a barrier of 5.0 kcal mol^{-1}. The dimer model (Figure 7, Figure 9) is a first and crude approximation of the situation in a monolayer. The STM images indicate a more complex arrangement of the dipolar rotors on the surface. For a more details regarding the method applied, see Supporting Information.

Conclusion

The synthesis of four new functionalized TOTA platform compounds was reported, of which **1 a**–**c** contain dipolar rotor units on top and **1 d** serving as a reference compound for STM investigations. The molecules were designed in such a way that the platforms absorb on metal surfaces, forming self-assembled arrays of free standing azimuthal dipolar rotors that interact through electrostatic dipole dipole interactions.

Compound **1 a** with the highest dipole moment (4.24 D) was sublimed onto Ag(111) surfaces and the self-assembled monolayers were investigated by STM. The STM images indicate a well-ordered but complex absorption pattern.

Theoretical calculations predict strong electrostatic interactions between neighboring dipolar rotors. The attractive Coulomb forces are sufficiently strong to force the otherwise upright standing axes of neighboring molecules to bend towards each other to form intermolecular H bonds between the pyridazine rotors. The rotational barrier of the dipolar units in an H bonded dimer is calculated as 5 kcal mol^{-1}. The situation

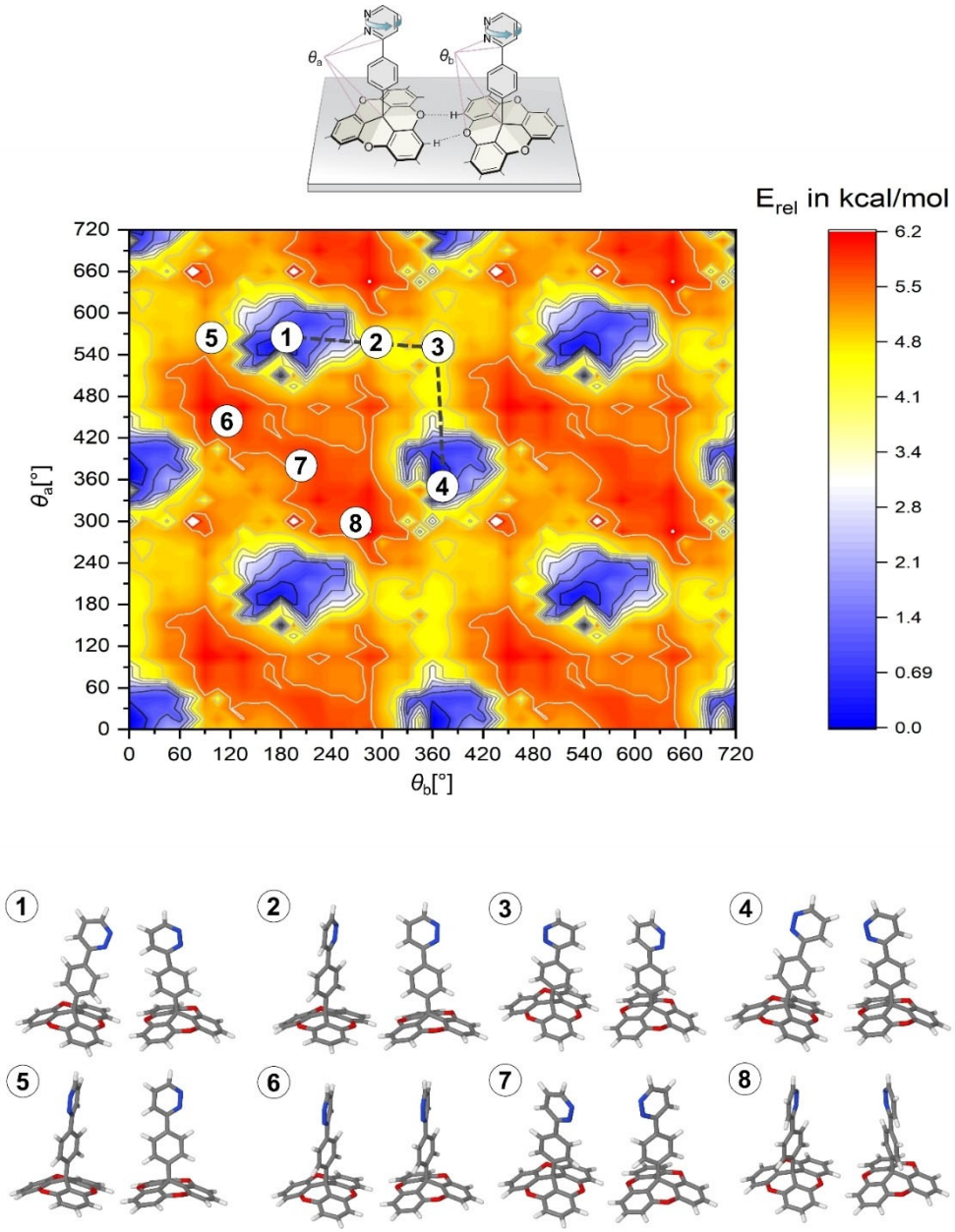

Figure 9. Energy hypersurface (PBE/def2SVP (DSPD3-BJ) of a dipolar rotor dimer (1a dimer) as a function of the two torsional angles θ_a *and* θ_b at a platform distance of $d = 9.1$ Å. The two platforms are fixed on a virtual surface, the torsional angles θ_a *and* θ_b are varied in steps of 15° and all other parameters are optimized. The energy hypersurface without boundaries has the topology of a torus. For a more comprehensible visualization four energy hypersurfaces with $\theta_a = 0$–$360°$, $\theta_b = 0$–$360°$ joint together to represent a surface with $\theta_a = 0$–$720°$, $\theta_b = 0$–$720°$. The lowest energy path between two minima (head-to-tail arrangements, in deep blue) is represented with a dashed line. Structures of the stationary points (minima, transition states and hill tops) are assigned to numbers 1–8 (for more information, see the Supporting Information, p. 34).

certainly is more complicated if all rotors in a 2D arrangement will be included. This will be subject of future investigations.

Acknowledgements

We are grateful for support by the Deutsche Forschungsgemeinschaft through SPP 1928 and SFB 677. Open Access funding enabled and organized by Projekt DEAL.

Conflict of Interest

The authors declare no conflict of interest.

Keywords: dipolar rotors · pyridazines · scanning tunneling microscopy · surfaces · trioxatriangulene (TOTA) platforms

[1] V. Balzani, A. Credi, F. M. Raymo, J. F. Stoddart, *Angew. Chem. Int. Ed.* **2000**, *39*, 3348–3391; *Angew. Chem.* **2000**, *112*, 3484–3530.

[2] W. R. Browne, B. L. Feringa, *Nat. Nanotechnol.* **2006**, *1*, 25–35.
[3] S. Kassem, T. van Leeuwen, A. S. Lubbe, M. R. Wilson, B. L. Feringa, D. A. Leigh, *Chem. Soc. Rev.* **2017**, *46*, 2592–2621.
[4] J. Frank, *Molecular Machines in Biology: Workshop of the Cell*, Cambridge University Press, Cambridge, **2011**.
[5] R. Horansky, T. Magnera, J. Price, J. Michl in *Lecture Notes in Physics. Controlled Nanoscale Motion. Artificial Dipolar Molecular Rotors, Vol. 711* (Eds: H. Linke, A. Månsson), Springer, Berlin, Heidelberg, **2007**, pp. 303–330.
[6] B. P. Abolins, R. E. Zillich, K. B. Whaley, *J. Chem. Phys.* **2018**, *148*, 102338.
[7] I. J. S. De Vlugt, D. Iouchtchenko, E. Merali, P.-N. Roy, R. G. Melko, *Phys. Rev. B* **2020**, *102*, 035108.
[8] U. G. E. Perera, F. Ample, H. Kersell, Y. Zhang, G. Vives, J. Echeverria, M. Grisolia, G. Rapenne, S.-W. Hla, *Nature Nanotech* **2013**, *8*, 46–51.
[9] Y. Zhang, J. P. Calupitan, T. Rojas, R. Tumbleson, G. Erbland, C. Kammerer, T. M. Ajayi, S. Wang, L. A. Curtis, A. T. Ngo, S. E. Ulloa, G. Rapenne, S.-W. Hla, *Nat. Commun.* **2019**, *10*, 3742.
[10] T. Ye, T. Takami, R. Wang, J. Jiang, P. S. Weiss, *J. Am. Chem. Soc.* **2006**, *128*, 10984–10985.
[11] T. Takami, T. Ye, D. P. Arnold, K. Sugiura, R. Wang, J. Jiang, P. S. Weiss, *J. Phys. Chem. C* **2007**, *111*, 2077–2080.
[12] J. Otsuki, Y. Komatsu, D. Kobayashi, M. Asakawa, K. Miyake, *J. Am. Chem. Soc.* **2010**, *132*, 6870–6871.
[13] H. Tanaka, T. Ikeda, M. Takeuchi, K. Sada, S. Shinkai, T. Kawai, *ACS Nano* **2011**, *5*, 9575–9582.
[14] K. H. A. Yeung, T. Kühne, F. Eisenhut, M. Kleinwächter, Y. Gisbert, R. Robles, N. Lorente, G. Cuniberti, C. Joachim, G. Rapenne, C. Kammerer, F. Moresco, *J. Phys. Chem. Lett.* **2020**, *11*, 6892–6899.
[15] L. Gao, Q. Liu, Y. Y. Zhang, N. Jiang, H. G. Zhang, Z. H. Cheng, W. F. Qiu, S. X. Du, Y. Q. Liu, W. A. Hofer, H.-J. Gao, *Phys. Rev. Lett.* **2008**, *101*, 197209.
[16] Y. Zhang, H. Kersell, R. Stefak, J. Echeverria, V. Iancu, U. G. E. Perera, Y. Li, A. Deshpande, K.-F. Braun, C. Joachim, G. Rapenne, S.-W. Hla, *Nat. Nanotechnol.* **2016**, *11*, 706–712.
[17] J. Vacek, J. Michl, *PNAS* **2001**, *98*, 5481–5486.
[18] D. Horinek, J. Michl, *J. Am. Chem. Soc.* **2003**, *125*, 11900–11910.
[19] T. Frauhammer, L. Gerhard, K. Edelmann, M. Lindner, M. Valášek, M. Mayor, W. Wulfhekel, *Phys. Chem. Chem. Phys.* **2021**, *23*, 4874–4881.
[20] J. Michl, E. C. H. Sykes, *ACS Nano* **2009**, *3*, 1042–1048.
[21] B. Baisch, D. Raffa, U. Jung, O. M. Magnussen, C. Nicolas, J. Lacour, J. Kubitschke, R. Herges, *J. Am. Chem. Soc.* **2009**, *131*, 442–443.
[22] S. Kuhn, B. Baisch, U. Jung, T. Johannsen, J. Kubitschke, R. Herges, O. Magnussen, *Phys. Chem. Chem. Phys.* **2010**, *12*, 4481–4487.
[23] S. Kuhn, U. Jung, S. Ulrich, R. Herges, O. Magnussen, *Chem. Commun.* **2011**, *47*, 8880–8882.
[24] T. Jasper-Toennies, M. Gruber, S. Ulrich, R. Herges, R. Berndt, *Angew. Chem. Int. Ed.* **2020**, *59*, 7008–7017; *Angew. Chem.* **2020**, *132*, 7074–7083.
[25] A. Schlimm, R. Löw, T. Rusch, F. Röhricht, T. Strunskus, T. Tellkamp, F. Sönnichsen, U. Manthe, O. Magnussen, F. Tuczek, R. Herges, *Angew. Chem. Int. Ed.* **2019**, *58*, 6574.
[26] H. Jacob, S. Ulrich, U. Jung, S. Lemke, T. Rusch, C. Schütt, F. Petersen, T. Strunskus, O. Magnussen, R. Herges, F. Tuczek, *Phys. Chem. Chem. Phys.* **2014**, *16*, 22643.
[27] T. R. Rusch, M. Hammerich, R. Herges, O. M. Magnussen, *Chem. Commun.* **2019**, *55*, 9511.
[28] T. R. Rusch, A. Schlimm, N. R. Krekiehn, T. Tellkamp, Š. Budzák, D. Jacquemin, F. Tuczek, R. Herges, O. M. Magnussen, *Angew. Chem. Int. Ed.* **2020**, *59*, 17192–17196; *Angew. Chem.* **2020**, *132*, 17345–17349.
[29] T. Tellkamp, J. Shen, Y. Okamoto, R. Herges, *Eur. J. Org. Chem.* **2014**, 5456–5461.
[30] R. Löw, T. Rusch, F. Röhricht, O. Magnussen, R. Herges, *Beilstein J. Org. Chem.* **2019**, *15*, 1485–1490.
[31] T. Jasper-Toennies, A. Garcia-Lekue, T. Frederiksen, S. Ulrich, R. Herges, R. Berndt, *J. Phys. Condens. Matter* **2019**, *31*, 18LT01.
[32] R. Löw, T. Rusch, T. Moje, F. Röhricht, O. M. Magnussen, R. Herges, *Beilstein J. Org. Chem.* **2019**, *15*, 1815–1821.
[33] T. Jasper-Toennies, M. Gruber, S. Johannsen, T. Frederiksen, A. Garcia-Lekue, T. Jäkel, F. Röhricht, R. Herges, R. Berndt, *ACS Nano* **2020**, *14*, 3907–3916.
[34] J. Strueben, M. Lipfert, J.-O. Springer, C. A. Gould, P. J. Gates, F. D. Sönnichsen, A. Staubitz, *Chem. Eur. J.* **2015**, *21*, 11165–11173.
[35] B. U. W. Maes, S. Verbeeck, T. Verhelst, A. Ekomié, N. von Wolff, G. Lefèvre, E. A. Mitchell, A. Jutand, *Chem. Eur. J.* **2015** *21*, 7858–7865.
[36] TURBOMOLE V7.2 **2017**, a development of University of Karlsruhe and Forschungszentrum Karlsruhe GmbH, 1989–2007, TURBOMOLE GmbH, since 2007; available from http://www.turbomole.com.

Manuscript received: September 6, 2021
Accepted manuscript online: October 19, 2021
Version of record online: November 5, 2021

